Biochimica et Biophysica Acta 1814 (2011) 638–646

Contents lists available at ScienceDirect

Biochimica et Biophysica Acta

journal homepage: www.elsevier.com/locate/bbapap

Structural and enzyme activity studies demonstrate that aryl substituted 2,3-butadienamine analogs inactivate *Arthrobacter globiformis* amine oxidase (AGAO) by chemical derivatization of the 2,4,5-trihydroxyphenylalanine quinone (TPQ) cofactor ☆

Karin Ernberg [a], Bo Zhong [b,1], Kristin Ko [c,1], Larry Miller [d,1], Yen Hoang le Nguyen [a], Lawrence M. Sayre [e,2], J. Mitchell Guss [a,*], Irene Lee [e,**]

[a] School of Molecular Bioscience, The University of Sydney, NSW 2006, Australia
[b] Department of Chemistry, Cleveland State University, Cleveland, OH 44115, USA
[c] Department of Chemistry, University of Michigan, Ann Arbor, MI 48109, USA
[d] Department of Chemistry, Westminster College, New Wilmington, PA 16172, USA
[e] Department of Chemistry, Case Western Reserve University, Cleveland, OH 44106, USA

ARTICLE INFO

Article history:
Received 2 November 2010
Received in revised form 23 December 2010
Accepted 30 December 2010
Available online 6 January 2011

Keywords:
Allenic amine
Arthrobacter globiformis amine oxidase
Mechanism-based inactivator
Crystal structure
Inhibition potency

ABSTRACT

Copper amine oxidases (CAOs) are a family of redox active enzymes containing a 2,4,5-trihydroxyphenylalanine quinone (TPQ) cofactor generated from post translational modification of an active site tyrosine residue. The *Arthrobacter globiformis* amine oxidase (AGAO) has been widely used as a model to guide the design and development of selective inhibitors of CAOs. In this study, two aryl 2,3-butadienamine analogs, racemic 5-phenoxy-2,3-pentadienylamine (POPDA) and racemic 6-phenyl-2,3-hexadienylamine (PHDA), were synthesized and evaluated as mechanism-based inactivators of AGAO. Crystal structures show that both compounds form a covalent adduct with the amino group of the substrate-reduced TPQ, and that the chemical structures of the rac-PHDA and rac-POPDA modified TPQ differ by the allenic carbon that is attached to the cofactor. A chemical mechanism accounting for the formation of the respective TPQ derivative is proposed. Under steady-state conditions, no recovery of enzyme activity is detected when AGAO pre-treated with rac-PHDA or rac-POPDA is diluted with excess amount of the benzylamine substrate (100-fold K_m). Comparing the IC_{50} values further reveals that the phenoxy substituent in POPDA offers an approximately 4-fold increase in inhibition potency, which can be attributed to a favourable binding interaction between the oxygen atom in the phenoxy group and the active site of AGAO as revealed by crystallographic studies. This hypothesis is corroborated by the observed >3-fold higher partition ratio of PHDA compared to POPDA. Taken together, the results presented in this study reveal the mechanism by which aryl 2,3-butadienamines act as mechanism-based inhibitors of AGAO, and the potency of enzyme inactivation could be fine-tuned by optimizing binding interaction between the aryl substituent and the enzyme active site.

1. Introduction

Copper amine oxidases (CAOs) are a family of redox active enzymes that catalyze the oxidative deamination of primary amines to aldehydes, with concomitant reduction of O_2 to H_2O_2 (Scheme 1 [1–3]). CAOs are nearly ubiquitous in nature, as they are found in plants, most yeasts, microorganisms, and mammals but somewhat surprisingly not in archaea. Most CAOs contain a 2,4,5-trihydroxyphenylalanine quinone (TPQ) cofactor, which is derived from the post-translational modification of an active site tyrosine residue [4–5]. During enzyme catalysis, the primary amine substrate condenses with TPQ to form a substrate Schiff base adduct (SSB). The SSB then tautomerizes to a product Schiff base (PSB), which upon hydrolysis affords a reduced aminated TPQ (TPQ_{amr})

Abbreviations: CAO, copper-containing amine oxidase; AGAO, *Arthrobacter globiformis* amine oxidase; PHDA, racemic 6-phenyl-2,3-hexadienylamine; POPDA, racemic 5-phenoxy-2,3-pentadienylamine; PSB, product Schiff base; SSB, substrate Schiff base; TPQ, trihydroxyphenylalanine quinone

☆ This work was supported in part by a grant from NIH (GM 48812) and an award from the American Diabetes Association (1-06-RA-117) to L.M.S. and I.L., and by a Linkage grant from the Australian Research Council (LP0669658) to J.M.G.

* Corresponding author: Tel.: +61 2 9351 4302; fax: +61 2 9351 5858.
** Corresponding author: Tel.: +1 216 368 6001; fax: +1 216 368 3006.
E-mail addresses: Mitchell.guss@sydney.edu.au (J.M. Guss), IXL13@case.edu (I. Lee).

[1] Present address.
[2] In memory of Professor Lawrence M. Sayre, July 25, 1951 to May 8, 2009.

1570-9639/$ – see front matter © 2011 Elsevier B.V. All rights reserved.
doi:10.1016/j.bbapap.2010.12.016

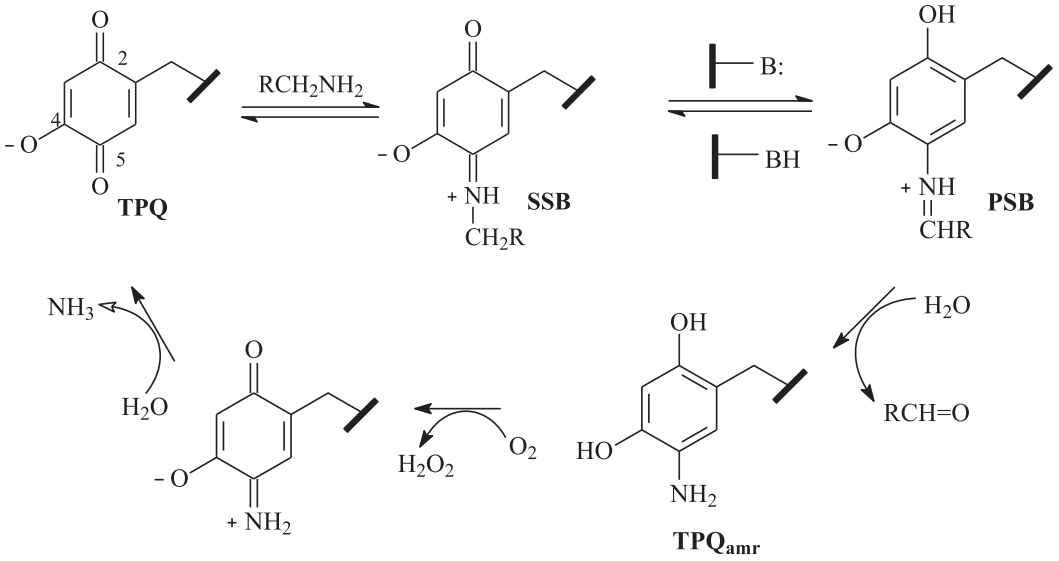

Scheme 1. Proposed mechanism for the TPQ-catalyzed oxidation of primary amine in copper amine oxidases.

and an aldehyde. These events are collectively known as the reductive half-reaction. In the oxidative half-reaction, the TPQ_{amr} is oxidized by O_2 to form quinonimine, which then undergoes hydrolysis to release ammonia to regenerate the TPQ cofactor.

In designing selective inhibitors against CAOs, a mechanism-based strategy targeting the reductive half-reaction has been exploited [6]. In particular, the approach of incorporating an electrophile adjacent to the substrate amino group in primary amines containing an aromatic group led to the synthesis of 4-aryloxy 2-butynamines as selective mechanism-based inhibitors [7]. Previous crystallographic studies of AGAO treated with two 4-aryloxy-2-butynamine analogs revealed a mechanism of enzyme inactivation involving covalent attachment of the α,β-unsaturated aldehyde turnover product generated from amine substrate oxidation to the amino group of TPQ_{amr} derived from the first half-reaction.

To further investigate the kinds of electrophile that can be used to design mechanism-based inhibitors of CAOs, two aryl 2,3-butadienamine analogs, racemic 5-phenoxy-2,3-pentadienylamine (POPDA) and racemic 6-phenyl-2,3-hexadienylamine, (PHDA, Fig. 1) were synthesized. These two compounds contain the 1-amino-2,3-butadiene moiety that has been shown by Qiao and coworkers to inactivate bovine plasma amine oxidase (BPAO) with higher potency compared to 1-amino-3-butyne amine [8]. As aromatic amines containing the 1-amino-3-butyne amine moiety are mechanism-based inactivators of AGAO, it is plausible that rac-PHDA and rac-POPDA will inhibit AGAO. To test this hypothesis, the crystal structures of AGAO treated with rac-PHDA and rac-POPDA, as well as the enzyme inhibition profiles were determined. The findings presented in this study provide a structural framework to guide the design of enzyme selective mechanism-based allenic amine inhibitors for the respective enzyme that may benefit pharmaceutical developments.

2. Materials and methods

2.1. Synthesis of racemic 6-phenyl-2,3-hexadienylamine hydrochloride (PHDA)

A dioxane solution of the t-boc protected propargylamine was refluxed with 3-phenylpropanal, diisopropylamine and freshly prepared CuBr under Argon for 12 h using the method reported in by Casara et al [9]. The reaction was then quenched with 1 N acetic acid followed by extraction with diethyl ether. The organic layer was dried with anhydrous Na_2SO_4, prior to rotary evaporation under reduced pressure. The resulting crude reaction mixture was purified by silica gel flash chromatography to produce the t-boc protected 6-phenyl-hexa-2,3-dienylamine. The t-boc group was deprotected with 3 N HCl at room temperature. Removal of the solvent in excess HCl under vacuum afforded 1-amino-2,3-hexadiene hydrochloride with an overall 20% yield. ^{1}H NMR spectra were obtained using aVarian 400 MHz spectrometers with the chemical shifts being referenced to TMS or the solvent peak. ^{1}H NMR (CD_3OD) δ 7.24 (5H, m), 5.46 (1H, m), 5.29 (1H, m), 3.39 (2H, broad multiplet), 2.75 (2H, m), 2.38 (2H, m); ^{13}C NMR ($CDCl_3$) 206.25, 142.75, 129.74, 129.49, 127.14, 95.22, 86.06, 39.69, 36.20, 31.24; HRFABMS MH^+ m/z observed 174.12804, $C_{12}H_{16}N$ calculated 174.12827.

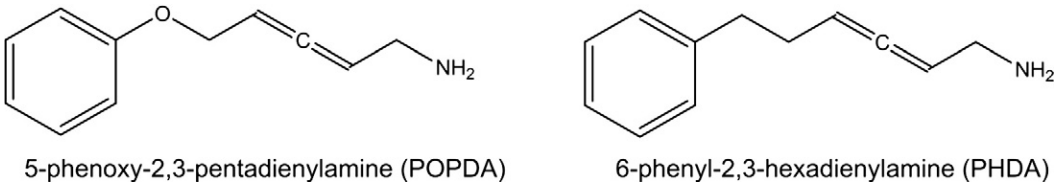

Fig. 1. Chemical structure of 5-phenoxy-2,3-pentadienylamine (POPDA) and 6-phenyl-2,3-hexadienylamine (PHDA). These two compounds were synthesized as described in Materials and methods as a racemic mixture. Both compounds first act as substrates to reduce the TPQ cofactor in AGAO and then chemically modify the reduced TPQ cofactor to inactivate enzyme turnover.

2.2. Synthesis of racemic 5-phenoxy-2,3-pentadienylamine (POPDA)

5-phenoxy-2,3-pentadienylamine was prepared via the custom synthesis service of Sai Pharmaceutical, Inc. using the same procedure previously described for the preparation of PHDA, except 2-phenoxyacetaldehyde was used to react with t-boc protected propargylamine. The identity of the final product was confirmed by liquid chromatography mass spectrometry (supplementary S1), infrared spectroscopy (supplementary S2) and ^{1}H NMR (500 MHz; DMSO-D_6; supplementary S3). The melting point of the product is 128.1 °C.

Prior to co-crystallization with purified AGAO, the inhibitors PHDA and POPDA were dissolved in 20% ethanol to give a final concentration of 100 mM. During protein work, the ethanol concentration was kept below 1% to avoid disrupting protein integrity.

2.3. Enzyme purification and crystallization

AGAO was overexpressed as a C-terminal Strep-tagII fusion protein and purified according to previous protocols [10], with an added final gel filtration step using a Sepharose 12 column. The protein was eluted with a solution of 0.1 M Tris–HCl and 0.3 M NaCl at pH 7.1 and subsequently concentrated to a final concentration of 12.9 mg mL^{-1} using a 30 kDa MWCO spin column (Millipore). Co-crystals of protein–inhibitor complexes were grown by vapor-diffusion in hanging drops at 293 K. Drops contained 2 μL reservoir solution (150 mM NaCitrate pH 7.0, 800 mM $(NH_4)_2SO_4$), 2 μL purified protein (12.9 mg mL^{-1}) and inhibitor (4 mM) and were set up over the reservoir. Crystals were obtained after two months.

2.4. X-ray data collection and analysis

The crystals were cryoprotected prior to data collection by 5% (v/v) incremental increases of glycerol to reach a final concentration of 30% (v/v) and immediately cryocooled in a stream of nitrogen at 100 K. X-ray diffraction data were collected using an in-house Rigaku RU200 generator (Rigaku, The Woodlands, USA) equipped with a copper rotating anode target ($\lambda = 1.5418$ Å) and Osmic mirror optics, and recorded on a Mar345 image plate detector (Marresearch). The data were processed using *DENZO* and *SCALEPACK* [11].

A previously refined AGAO model at 1.73 Å (PDB code 1SIH [7]) was used as the initial model for both AGAO/inhibitor structures. Solvent molecules, metal ions, sulfate ions, glycerol molecules and the TPQ/inhibitor complex were stripped from the model and residue 382 (TPQ) was initially modeled as alanine. Refinement was carried out using *REFMAC5* [12] within the *CCP4* program suite [13], with checks of the electron density maps ($F_{obs} - F_{calc}$ and $2F_{obs} - F_{calc}$) and manual modeling in *COOT* [14]. TLS refinement was used for AGAO/POPDA with one TLS group per subunit [15]. Inhibitors were built using the *Dundee PRODRG Server* [16].

Validation of the final structures was carried out using several complementary programs: the *MOLPROBITY* server [17] for geometric analysis of the model; *SFCHECK* [18] in the *CCP4* suite for model vs. data analysis; and, *POLYGON* [19] for comparison with structures of similar resolution.

2.5. Inhibition kinetics of AGAO by PHDA and POPDA

Using the generation of benzylaldehyde as an activity reporter of AGAO, the inhibition parameters of PHDA and POPDA were determined by monitoring the time courses of benzylamine oxidation in the presence of various concentrations of PHDA or POPDA [6]. The enzyme used in the kinetic studies was provided by the Dooley lab at the Montana State University. The steady-state rates were determined from tangents to the linear steady-state portions of the reaction time courses using the computer program KaleidaGraph (Synergy, Inc.). All experiments were performed at least in triplicate. Ratios of the initial rates of inhibited versus uninhibited (v_i/v_o) AGAO-catalyzed oxidation of 1 mM benzylamine were plotted against the corresponding rac-PHDA or rac-POPDA concentrations; fitting the plots with Eq. (1) generated the IC_{50} values (concentration of inhibitor needed to attain 50% enzyme inhibition), where [I] is the concentration of inhibitor, and n is the Hill coefficient (>1) introduced to fit the data.

$$\frac{vi}{vo} = \frac{1}{\left(1 + \frac{[I]^n}{IC50^n}\right)} \quad (1)$$

Table 1
X-ray data statistics. Values for outer shell are given in parentheses.

	AGAO/POPDA	AGAO/PHDA
Radiation wavelength (Å)	1.54178	
Space group	*C*2	
Unit-cell parameters		
a, *b*, *c* (Å)	192.7, 63.0, 158.2	157.9, 63.3, 92.2
β (°)	117.4	112.1
No. of molecules in ASU	2	1
Resolution range (Å)	50.00–1.90 (1.97–1.90)	50.00–2.050 (2.12–2.05)
No. of unique reflections	131273 (13143)	52557 (5229)
Completeness (%)	98.9 (99.7)	99.2 (99.4)
Redundancy	3.8 (3.6)	4.3 (3.9)
$I/\sigma(I)$	10.0 (3.5)	10.0 (2.9)
R_{merge}	0.078 (0.356)	0.091 (0.457)
Matthews coefficient, V_M (Å^3 Da^{-1})	2.96	2.97
Solvent content (%)	58	59

2.6. Time-dependent inhibition of AGAO by PHDA and POPDA

AGAO (2.5 μM) was incubated with 0-, approximately 5-, 10-, and 15-times the IC_{50} of PHDA or POPDA at 30 °C in 50 mM sodium phosphate, pH 7.2 for 0, 2, 5, 15 and 30 min prior to diluting 10-fold into 5 mM benzylamine in the phosphate reaction buffer. Upon dilution, the rates of benzylamine oxidation were monitored at 250 nm. The percentage enzyme activity remaining after inhibition was defined by dividing the rate of reaction containing inhibitor with the rate of uninhibited reaction at each time point. The partition ratios (*r*) for PHDA and POPDA were obtained by plotting the fractional

Table 2
Crystallographic refinement statistics. Values for outer shell are given in parentheses.

	AGAO/POPDA	AGAO/PHDA
No. of reflections used in refinement for R_{cryst}	124675 (8967)	49890 (3529)
No. of reflections for R_{free}	6538 (438)	2660 (169)
Average *B* factors		
Protein atoms (Å^2)	24.4	34.3
Solvent molecules (Å^2)	32.5	40.5
Metal ions (Å^2)	25.5	31.6
TPQ side chain (Å^2)	38.6	44.8
Final model		
Total no. of atoms	10715	5882
Protein residues	1235	618
Residues with alternate confomers	11	8
Metal ions	2 Cu, 2 Na	1 Cu, 1 Na
Sulfate ions	4	1
Glycerol molecules	10	11
R_{cryst}	0.176 (0.230)	0.178 (0.305)
R_{free}	0.218 (0.280)	0.221 (0.343)
Ramachandran data		
Allowed (%)	99.8	99.8
Favored (%)	97.1	96.7
Outliers (%)	0.2	0.2
R.m.s.d. from ideal geometry		
Bond lengths (Å^2)	0.01	0.01
Bond angles (°)	1.5	1.5
PDB ID	3KII	3KN4

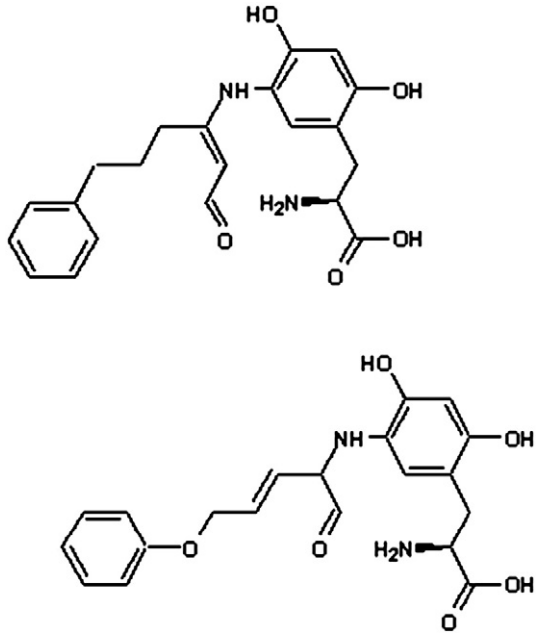

Fig. 2. Chemical structures of the complex formed between the reduced TPQ and inhibitor as revealed by the respective crystal structure of enzyme-inhibitor complex. Top: TPQ/PHDA. Bottom: TPQ/POPDA.

enzyme velocity, defined by dividing the percentage enzyme activity remaining with and without inhibitor treatment, against the corresponding [I]/[AGAO] ratio. The *r* value was determined by subtracting 1 from the intercept on the 'fractional enzyme velocity' axis obtained by extrapolating a straight line fit of the data.

3. Results and discussion

The structures of AGAO in complex with PHDA and POPDA were refined to 2.05 and 1.90 Å resolution, respectively. X-ray data collection and refinement statistics can be found in Tables 1 and 2. Overall the structure of AGAO is not significantly different from that found in crystals of the native enzyme. The r.m.s.d. for C^{α} atoms between either of the complexes reported in this paper and the native structures previously reported (PDB codes 1W6G and 1W6C [20]) range from 0.2 to 0.4 Å. Four other structures of AGAO with a covalently bound inhibitor have been published (PDB codes 1SIH and 1SII [7], 1W4N and 1W5Z [21]). When compared with these models, the complexes reported here align with a slightly lower r.m.s.d for C^{α} atoms than when compared to native structures. This is expected since the active site residues move slightly upon substrate binding. The electron density maps for the AGAO/PHDA and the AGAO/POPDA complexes revealed both inhibitors to be covalently bound to the enzyme through the C5 carbon of the TPQ cofactor as reported previously for 4-aryloxy-2-butynamine compounds [7] as well as benzylhydrazine and tranylcypromine [21]. Overall, the active site cavities are very similar to each other in the two structures as well as to other AGAO inhibitor complexes [7,21]. The O5 atom on C5 of TPQ is modeled as a nitrogen atom, linking to the C^{γ} and C^{β} of PHDA and POPDA respectively (Fig. 2), and the chemical mechanism accounting for the formation of each adduct is presented in Scheme 2. As discussed below, the differences in the binding interaction between AGAO with rac-PHDA and rac-POPDA could cause the observed difference in adduct formed between the respective inhibitor and TPQ_{amr}. The B-factors of the inhibitors are slightly higher on average (~60 $Å^2$) than the surrounding residues, suggesting that the sites may not be fully occupied in either inhibitor complex. In the absence of an inhibitor, the TPQ in AGAO is normally disordered suggesting that any uncomplexed TPQ in the crystals would simply not be observed.

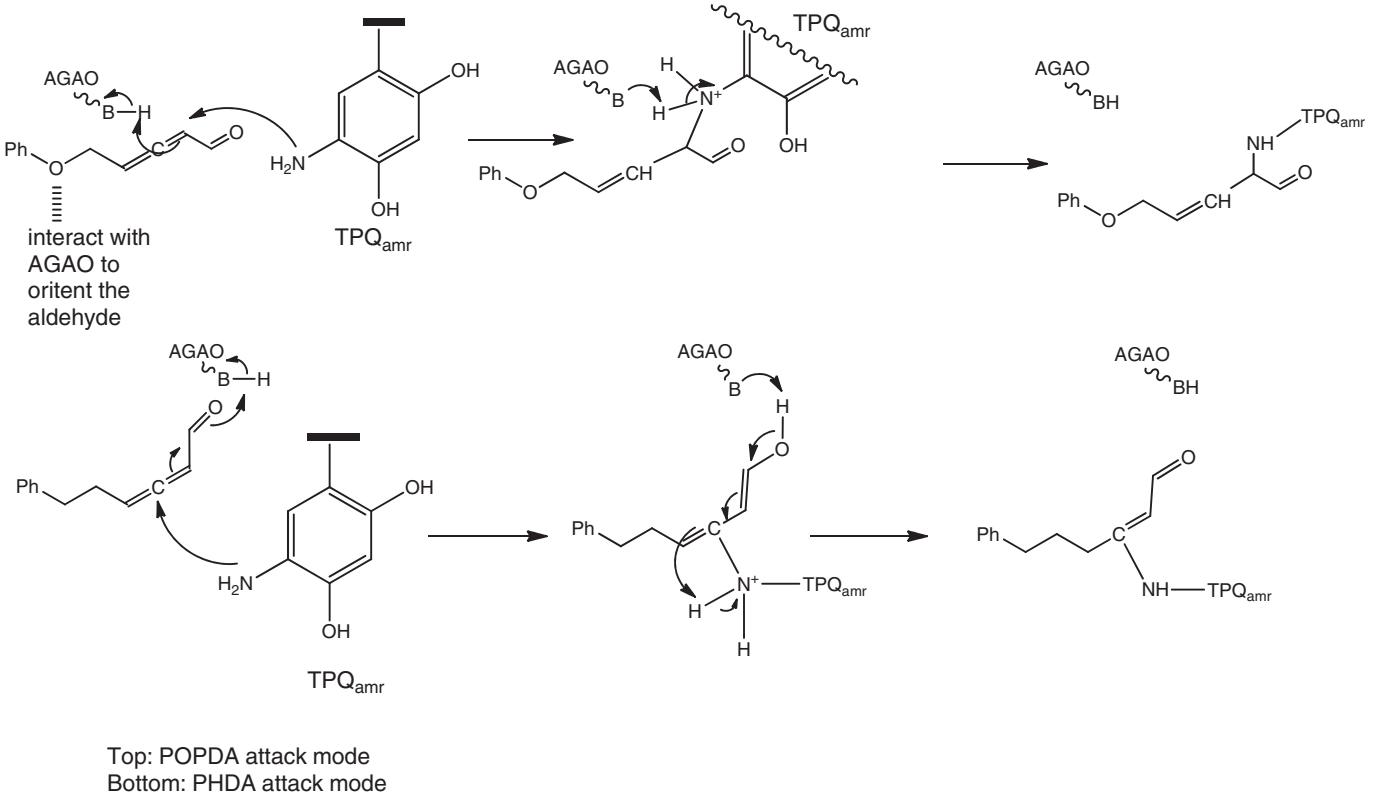

Scheme 2. Proposed mechanism for the inactivation of AGAP by POPDA (top) and PHDA (bottom).

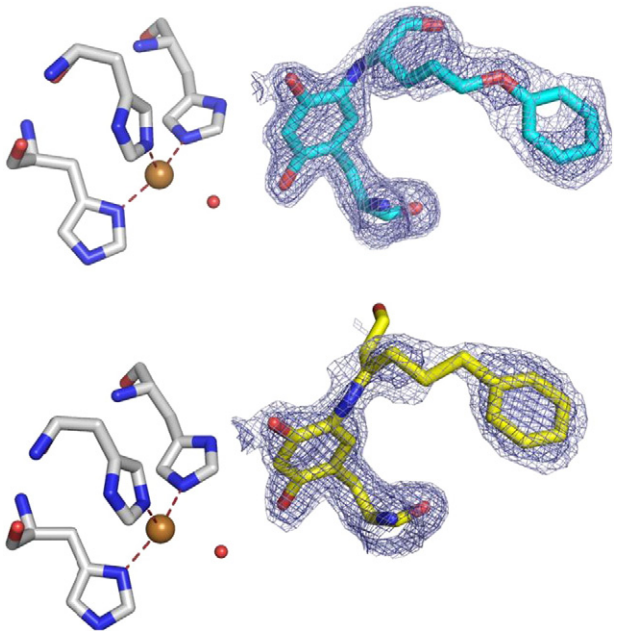

Fig. 3. The 2Fo–Fc map at 1.0 (light blue) and 1.5 (dark blue) sigma for TPQ/PHDA (yellow) and TPQ/POPDA B (blue). The active site copper is shown, coordinated by His 431, 433 and 592 and the water molecule linking the copper to the TPQ molecule.

3.1. TPQ and the active site

In both structures reported here, the TPQ cofactor is in its active "off-Cu" conformation (Fig. 3) which is required for adduct formation with the inhibitors. The copper atom is coordinated by three histidine residues, His 431, His 433 and His 592, and one water molecule. This water molecule also forms a hydrogen bond to the O2 atom of TPQ. There is no significant residual electron density for a second water molecule that is frequently observed to coordinate the copper atom in many other CAO structures. The position of the TPQ in its active conformation allows it to hydrogen bond via its O4 atom with the OH group of Tyr 284. Asn 381 tilts down towards the TPQ ring moiety, making contacts of ~3.5 Å between its O^{δ} and N^{δ} atoms and the C3 and C5 atoms of TPQ. This interaction combined with the hydrogen bonds effectively restricts the movement of the TPQ.

The shift of the TPQ from its inactive to its active conformation upon binding of the inhibitors is accompanied by the movement of the 'gate' residue, Tyr 296, which lies in the active site channel, to its "open" position [22], see Fig. 4. This ~90° rotation accommodates the TPQ/inhibitor adduct and has been observed for other inhibitor structures of AGAO [7,21,23]. This movement is accompanied by movements of Leu 137 and of the sidechain of Pro 136. In active "off-Cu" AGAO, the tyrosine is in its open conformation allowing access to the TPQ, whereas in inactive "on-Cu" AGAO, it is in a closed conformation blocking substrate access to the active site, hence its designation as a 'gate'. Interestingly, in AGAO/PHDA there is only poor electron density for Tyr 296 and the side chain has high B-factors, indicating that it is disordered. This can be compared to AGAO/POPDA where Tyr 296 has side chain B-factors of about 35–40 $Å^2$ in both subunits and is well ordered. The disorder of Tyr 296 in AGAO/PHDA is surprising and has only been observed in one other structure where the TPQ is ordered and in an "off-Cu" conformation (PDB code 1W6C, [20]). The movement of Pro 136, which results from inhibitor binding and the movement of Tyr 296, allows its carbonyl oxygen atom to form a hydrogen bond with Tyr 302 OH. The Tyr 296 O to Tyr 302 OH distance of ~2.9–3.0 Å compares with ~4 Å in the native structure.

3.2. Mode of inhibitor binding

The residues that line the cavity surrounding the inhibitors (< 3.5 Å), include Ile 379 and Gly 380 on the top side of the non-aromatic part of the substrate, Leu 137 and Tyr 296 below and Tyr 302 on the side (Fig. 5). Phe 407 lies on the opposite side of the wall facing Tyr 302. Other residues interact with the phenyl ring of the inhibitor molecules, including Phe 105 at the end of the inhibitor channel, Ala 135 and Pro 136 below the phenyl ring and Trp 168 on the side opposite Phe 105. Leu 358 and Trp 359 from the other subunit in the dimer lie at the very end of the channel and also interact with the inhibitor phenyl ring. The phenyl groups of the inhibitors extend out into the active site cavity between residues Pro 136 and Gly 380 (Fig. 5). The position of the inhibitor causes Phe 105 to move significantly (~45° rotation) in order to accommodate the large molecule in the active site, something that has been reported previously for similar large inhibitor molecules [7,21]. However, in AGAO/POPDA chain A as well as AGAO/PHDA, Phe 105 is disordered and not visible in the electron density maps.

For both inhibitors, the terminal amine group is modeled as an aldehyde, resulting from prior oxidation by the enzyme, consistent with the proposed reaction mechanism and previous reports [7,21,23,24]. However, in the structure of the PHDA complex, the electron density associated with the aldehyde group and adjacent atoms is very weak, which together with the very high B-factors, indicates that this "arm" is highly disordered and does not make any significant interactions with nearby protein residues. While it is clear that an adduct has formed with PHDA, disorder of Tyr 296, Phe 105 and the aldehyde end of the inhibitor, prevent a detailed discussion of

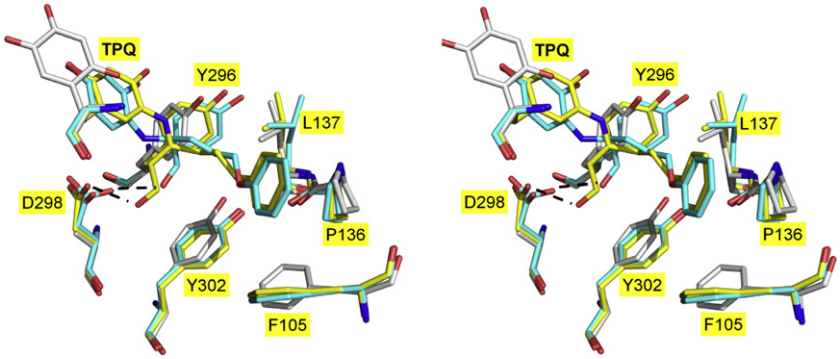

Fig. 4. The active site residues that have moved significantly upon inhibition are displayed for AGAO/PHDA (yellow), AGAO/POPDA (blue) and native protein (white, PDB ID 1W6G). When the protein is inactive, the TPQ is on-copper; whereas in active AGAO, the TPQ is off-copper. The change from on-copper TPQ to its off-position switches the active site gate reside Tyr 296 from a closed conformation to an open. This movement pushes Leu 137 and Pro 136 around, and allows Tyr 302 to interact with the backbone of Pro 136. Phe 105 moves in order to interact with the large phenyl ring of the inhibitor. Dashed lines indicate the interactions between the aldehyde arms of PHDA and POPDA and the catalytic base Asp 298.

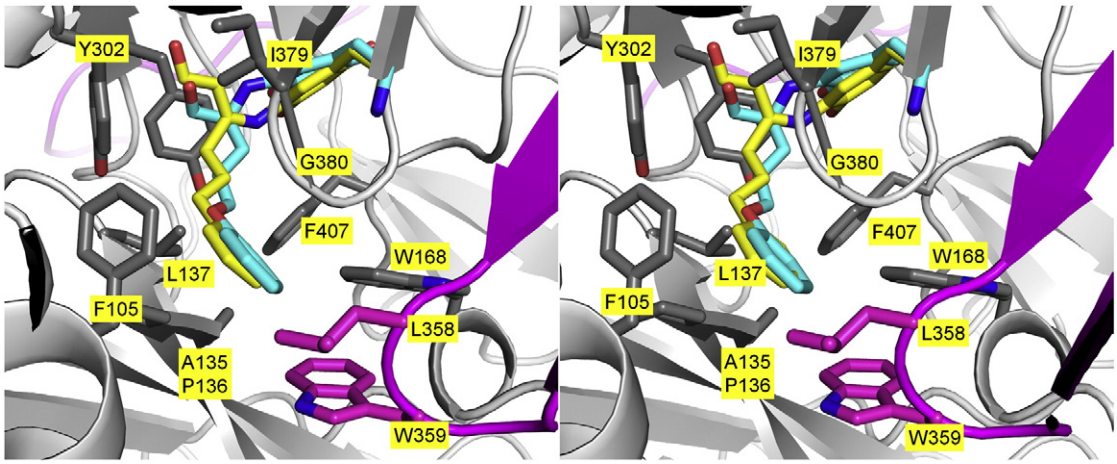

Fig. 5. TPQ/PHDA (yellow) and TPQ/POPDA (blue) interacts with mainly hydrophobic residues where it sits in the active site. A loop from the second subunit in the dimer reaches in and interacts with the inhibitor phenyl ring through residues 358 and 359 (magenta).

its interactions. In the complex with POPDA, however, the aldehyde moiety is clearly visible and interacts with Asp 298, the conserved catalytic base in the enzymatic reaction (Fig. 4). The interaction with the aldehyde "arm" in AGAO/POPDA causes a ~90° rotation of the side chain of Asp 298 in both subunits of AGAO/POPDA when compared to native structures and other inhibitor complexes. This movement allows Asp 298 to hydrogen bond to the aldehyde oxygen of POPDA with the consequence that the aspartate must be protonated. The second carboxyl oxygen atom of Asp 298 forms a hydrogen bond to Tyr 384 OH. The specific interaction between Asp 298 and the aldehyde arm of POPDA may help to retain the oxidized aldehyde product in the active site of AGAO, thereby facilitating the inactivation of TPQ_{amr} by the mechanism proposed in Scheme 2. Overall, the two AGAO inhibitor structure active sites are apparently very similar but the disorder seen in the PHDA complex indicates that there are fewer stabilizing interactions than in the POPDA complex. This observation would suggest that the ratio of aldehyde release to aldehyde retention would be higher in the PHDA complex than in the POPDA complex as discussed below in relation to the partition ratios.

3.3. Mode of enzyme inhibition

As indicated above PHDA and POPDA link to the TPQ by different carbon atoms; C^{γ} and C^{β} of PHDA and POPDA, respectively (Fig. 2). These different "attack modes" cause the inhibitor in AGAO/POPDA to stretch ~0.8 Å further out towards the opening of the active site cavity (Fig. 4). To account for the formation of the POPDA and PHDA derivatized TPQ, the mechanisms depicting the reaction between TPQ_{amr} with the aldehydes generated from oxidation of the respective compounds are proposed in Scheme 2. The two mechanisms differ by the position at which the C5 amino group of TPQ_{amr} attacks the electrophilic carbon in the allenic aldehydes generated from initial oxidation of the primary amine in the two compounds. The electrostatic potential maps of the allenic aldehydes generated from amine oxidation are shown in Fig. 6. The two structures differ principally by the orientation of the allenic aldehyde arms but not by electrophilicity at the β- and γ-carbons. Therefore, the observed differences in the mode of TPQ derivation could be attributed to the way by which the respective allenic group is positioned with respect to the C5 amino group of TPQ_{amr}. In POPDA, the phenoxy oxygen is surrounded by a hydrophilic patch in AGAO. The oxygen is replaced by a hydrophobic carbon in PHDA. Such interactions may position the aldehyde product of POPDA oxidation to react favorably at the β-carbon position as shown in the top panel of Scheme 2. The lack of such interactions in PHDA may allow a slightly different orientation of the diene in PHDA to favor nucleophilic attack of the TPQ_{amr} at the γ-carbon of the oxidized PHDA aldehyde product as proposed in the bottom panel of Scheme 2.

3.4. Potency of POPDA and PHDA as inhibitors of AGAO

Using benzylamine as substrate, the inhibitory effects of POPDA and PHDA on AGAO were compared by steady-state kinetic techniques. The fractional activity of AGAO activity determined in the presence of various concentrations of inhibitor was plotted against the corresponding inhibitor concentration to yield the dose–response curves shown in Fig. 7. Fitting the average data of each plot with Eq. (1) (see Materials and methods) provides an IC_{50} of 1.2 ± 0.1 μM for racemic POPDA. PHDA, which contains a methylene group rather than an ether oxygen juxtaposed to the phenyl ring, has an IC_{50} of 5.6 ± 0.3 μM, which is ~4-fold less potent than the aryloxy analog POPDA. When fitting the data to extract the IC_{50} values, the data shown in Fig. 7 fit best to Eq. (1), with an apparent Hill coefficient of 2.3 ± 0.3 for rac-PHDA, and 2.1 ± 0.3 for rac-POPDA. The data fits poorly if the Hill coefficient is set to one. As AGAO is a dimer, the Hill coefficient detected

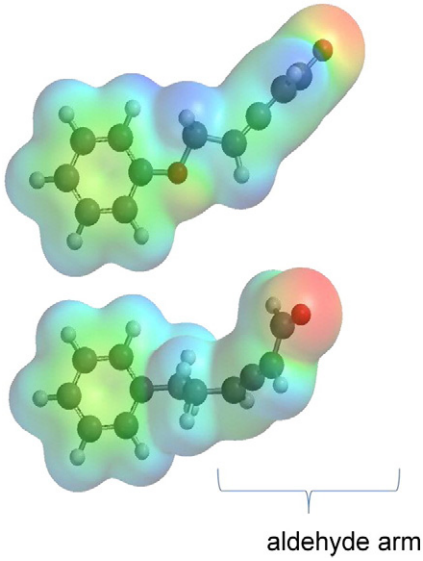

Fig. 6. Spartan models of the allenic aldehydes generated by the AGAO catalyzed oxidation of POPDA (*top*) and PHDA (*bottom*).

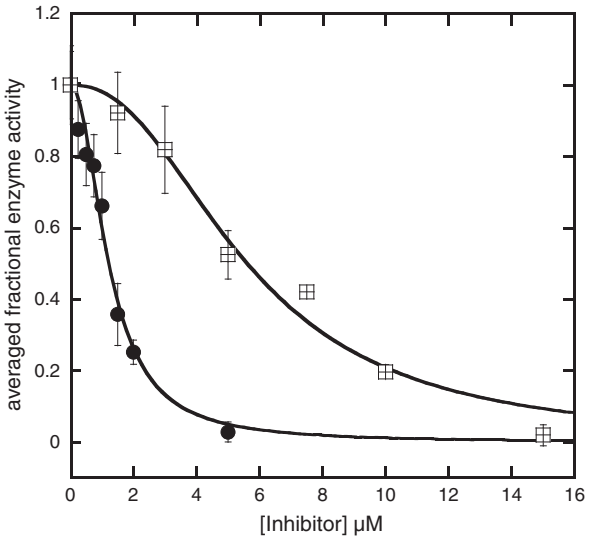

Fig. 7. Dose-dependent plot of the inhibition of AGAO by PHDA (□) and POPDA (●). All reactions were performed at least in triplicate. The fractional activities of AGAO-catalyzed the oxidation of benzylamine were determined by monitoring the formation of benzylaldehyde at 250 nm by UV spectroscopy as described in Materials and methods. The solid black line is the fit of the data with Eq. (1). All experimental values were within 25% or less deviation from the averaged values reported here.

Table 3

	Racemic PHDA	Racemic POPDA	4-phenyoxy-2-butyn-1-amine (PBA)
IC_{50} (μM)	5.6 ± 0.3	1.2 ± 0.1	50*
Partition ratio	52 ± 1	15.9 ± 0.9	12*

*Value obtained from O'Connell et al., Biochemistry 43, 10965–10978 (2004).

here reflects the extent of subunit communication during enzyme inhibition. However, the oxidation of benzylamine by AGAO is not cooperative [6]. Since benzylamine bears significant structural similarity with the inhibitors, it is not clear if the >1 Hill coefficient indeed reflects the level of cooperativity in AGAO. Additional studies will be needed to further clarify this issue. Alternatively, the apparent cooperativity can be attributed to the buildup of a certain amount of aldehyde product needed to inactivate AGAO. At low levels of allenic amine, the aldehyde product readily diffuses out of the enzyme active site whereas at high levels of the compound, enough of the aldehyde product is generated to stay bound and then inactivate the enzyme's TPQ_{amr}. At this time, the mechanistic feature giving rise to the observed Hill coefficient cannot be conclusively assigned. Therefore, additional work will be needed to define this issue.

According to the structural data described above, AGAO/POPDA is better-ordered in the electron density and displays interactions with active site residues (e.g. Asp 298) not observed in AGAO/PHDA. The disorder of Tyr 296 in AGAO/PHDA could further indicate less effective inhibitor binding (Fig. 5). The interactions observed between AGAO and POPDA are likely to provide a more productive binding mode in facilitating the modification of TPQ, which accounts for the lower IC_{50} of POPDA (Table 3). Fig. 2 shows the structures of TPQ modified by PHDA and POPDA. The mechanisms proposed for their formation are reminiscent of the one proposed for aryloxy-2-butyn-1-amines, which irreversibly inactivate AGAO by covalently modifying reduced TPQ through formation of an α,β-unsaturated aldehyde product. Therefore, experiments were conducted to evaluate whether AGAO is irreversibly inactivated by PHDA and POPDA. Fig. 8 shows the time courses of enzyme inactivation by different concentrations of PHDA or POPDA. In both cases, irreversible inactivation is indicated by the lack of recovery of activity upon dilution of the inhibitor-treated AGAO into 100-fold the K_m of benzylamine substrate [6], and by the completion of inactivation within 2 min of mixing with the inhibitors. These results are consistent with the mode of covalent enzyme inactivation revealed by the structures of the complexes. Furthermore, the inactivation appears to be completed within 2 min of reaction mixing, corroborating the observation that linear time courses were observed in the rac-PHDA and rac-POPDA treated reaction time courses (S4). It is likely that the chemical inactivation step was completed within the mixing timing of the reaction; the linear time courses detected the activity of the unreacted enzyme.

According to the mechanism proposed in Schemes 1 and 2, PHDA and POPDA will be converted to an α,β-unsaturated aldehyde product, which either diffuses out of the active site to enable subsequent enzyme turnover, or reacts with the reduced TPQ to

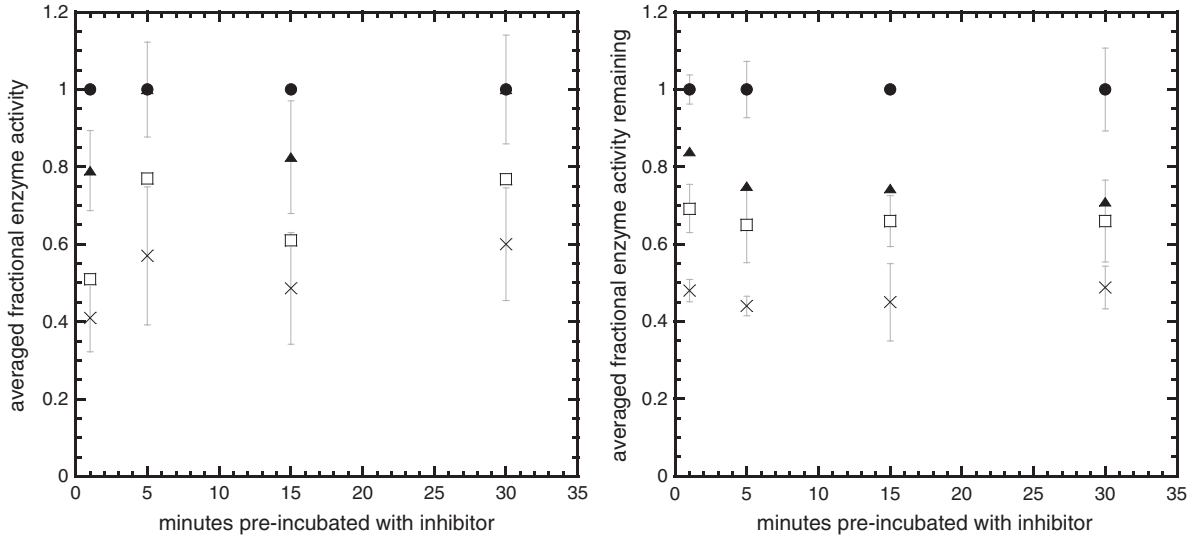

Fig. 8. Time courses of irreversible inactivation of AGAO by PHDA (left) and POPDA (right). AGAO (2.5 μM) was incubated with 0- (●), 22.5- (▲), 45- (□) and 67.5- (X) μM of PHDA or 0- (●), 7.5- (▲), 15- (□) and 22.5- (X) μM of POPDA for 0, 2, 5, 15 and 30 min prior to diluting 10-fold into 5 mM benzylamine in the phosphate reaction buffer as described in Materials and methods. Upon dilution, the rates of benzylamine oxidation were monitored at 250 nm. The percentage enzyme activity remaining is standardized against the rate of benzylaminie oxidation in the absence of inactivator. To reduce clattering of the plots, the error bars for the 22.5 μM of PHDA and 7.5 μM of POPDA, which are within 25% are not shown.

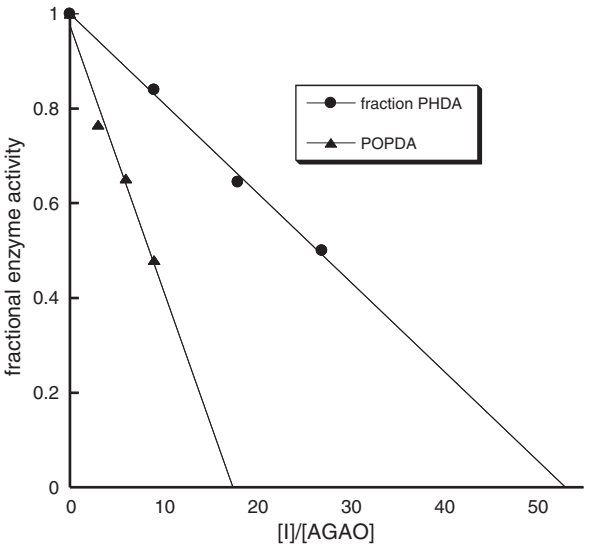

Fig. 9. Partition ration plot for the inactivation of AGAO by PHDA (●) and POPDA (▲). The fractional AGAO activity at the corresponding [I]/[AGAO] was determined by monitoring the oxidation of benzylamine to benzylaldehyde at 250 nm as described in Materials and method. In this plot, I represents PHDA or POPDA. All assays were performed at least in triplicates and experimental deviations were within 20% or less from the average fractional enzyme activity reported here. The partition ratio of the respective inactivator was extrapolated by subtracting 1 from the X-intercept of the corresponding compound.

render enzyme inactivation. The partition between the two processes can be quantified by the partition ratio, a value obtained by plotting residual enzyme activity with [I]/[E] as shown in Fig. 9. Fitting the data shown in Fig. 9 to a linear function generates the partition ratios for rac-PHDA and rac-POPDA (Table 3). For comparison, the partition ratio of 4-phenoxy-2-butyn-1-amine (PBA), which contains the same aryloxy substituent as POPDA, is included. It can be seen from Table 3 that the two inhibitors containing the phenoxy substituent have comparable partition coefficients, and that each is lower than the value found for rac-PHDA. The structural data shown in Figs. 4 and 5 reveal that the oxygen of the phenoxy group in POPDA could interact with Tyr 302 OH, Gly 380 N and Pro 136 O in AGAO, which are all within a distance of 4–5 Å. Since such interactions are not found in PHDA, it is possible that POPDA is more productively aligned with the amino group of reduced TPQ to facilitate the crosslinking reaction. Furthermore, the aldehyde product generated from POPDA oxidation may be better retained in the active site of AGAO due to the additional interactions between the phenoxy oxygen and the active site residues. This may account for the relatively lower partition ratio of POPDA (15.9) than PHDA (52).

4. Summary

CAOs are nearly ubiquitous enzymes that play important roles in the metabolism of amines in living organisms, including plants, yeast, microorganisms, and mammals. As such, potent and selective inhibitors of CAOs could benefit the development of antimicrobials, pesticides of plants or pharmaceuticals to treat human diseases. Therefore, the ability to rationally design selective CAO inhibitors based on available structural data should be beneficial. For example, the K_m of AGAO and BPAO catalyzed oxidation of benzylamine differs by 50-fold [6]. An understanding of the structural basis to account for the observed selectivity would shed light into the design of an appropriate substrate analog to deliver the inactivation motif such as the allenic amine moiety described in this study to inactivate the desirable enzyme homolog. Here, we presented structural and activity data to demonstrate that the two aromatic amines containing a 1-amino-2,3-butadiene functionality, PHDA and POPDA, are mechanism-based inhibitors of AGAO. These two compounds first act as substrates, which upon oxidation, become α,β-unsaturated aldehyde products that are highly reactive electrophiles. Consequently, the unsaturated aldehydes form a covalent adduct with the reduced TPQ cofactor (Scheme 2) to sequester the catalytic functions of AGAO, thereby eliminating enzyme turnover. Comparison of the structures of AGAO/PHDA and AGAO/POPDA complexes reveal binding interactions are present only in the latter enzyme complex. As POPDA is a more potent inhibitor than PHDA, with at least a 4-fold lower in IC_{50}, we attribute the observed potency to the binding interactions of POPDA by AGAO as revealed by the structural data. Furthermore, the phenoxy oxygen in POPDA contributes to a lower partition ratio in enzyme inhibition by interacting with a cluster of hydrophilic residues in the active site of AGAO. Taken together, this work demonstrates the utility of installing a 1-amino-2,3-butadiene unit as an electrophile in the design of potent mechanism-based inhibitors of AGAO. Given that the two inhibitors were generated and tested as a racemic mixture, it will be of interest to further determine if enzyme inhibition is also enantioselective. If so, the stereochemistry of allenic amines could be exploited as an additional parameter for future design of CAO inhibitors. Since unsubstituted 1-amino-2,3-butadiene inhibits other CAOs and monoamine oxidases, the results presented in this study should provide structural guidance in the design of selective and potent inhibitors for other oxidases.

Acknowledgement

We thank Edward Motea for assistance in the preparation of Fig. 6.

Appendix A. Supplementary data

Supplementary data to this article can be found online at doi:10.1016/j.bbapap.2010.12.016.

References

[1] S.M. Janes, M.M. Palcic, C.H. Scaman, A.J. Smith, D.E. Brown, D.M. Dooley, M. Mure, J.P. Klinman, Identification of topaquinone and its consensus sequence in copper amine oxidases, Biochemistry 31 (1992) 12147–12154.
[2] S.M. Janes, D. Mu, D. Wemmer, A.J. Smith, S. Kaur, D. Maltby, A.L. Burlingame, J.P. Klinman, A new redox cofactor in eukaryotic enzymes: 6-hydroxydopa at the active site of bovine serum amine oxidase, Science 248 (1990) 981–987.
[3] Y. Lee, L. Sayre, Model studies on the quinone-containing copper amine oxidases. Unambiguous demonstration of a transmination mechanism, J. Am. Chem. Soc. 117 (1995) 11823–11828.
[4] M. Mure, J. Klinman, Model studies of topaquinone-dependent amine oxidases. 2. Characterization of reaction intermediates and mechanism, J. Am. Chem. Soc. 117 (1995) 8707–8718.
[5] M. Mure, S. Millis, J. Klinman, Catalytic mechanism of the topa quinone containing copper amine oxidases, Biochemistry 41 (2002) 9269–9278.
[6] E.M. Shepard, J. Smith, B.O. Elmore, J.A. Kuchar, L.M. Sayre, D.M. Dooley, Towards the development of selective amine oxidase inhibitors. Mechanism-based inhibition of six copper containing amine oxidases, Eur. J. Biochem. 269 (2002) 3645–3658.
[7] K.M. O'Connell, D.B. Langley, E.M. Shepard, A.P. Duff, H.B. Jeon, G. Sun, H.C. Freeman, J.M. Guss, L.M. Sayre, D.M. Dooley, Differential inhibition of six copper amine oxidases by a family of 4-(aryloxy)-2-butynamines: evidence for a new mode of inactivation, Biochemistry 43 (2004) 10965–10978.
[8] C. Qiao, H. Jeon, L. Sayre, Selective inhibition of bovine plasma amine oxidase by homopropargylamine, a new inactivator motif, J. Am. Chem. Soc. 126 (2004) 8038–8045.
[9] P. Casara, K. Jund, P. Bey, General synthetic access to alpha-allenyl amine and alpha-allenyl-alpha-amino acids as potential enzyme-activated irreversible inhibitors of PLP-dependent enzymes, Tetranedron Lett. 25 (1984) 1891–1894.
[10] G.A. Juda, J.A. Bollinger, D.M. Dooley, Construction, overexpression, and purification of Arthrobacter globiformis amine oxidase–Strep-tag II fusion protein, Protein Expr. Purif. 22 (2001) 455–461.
[11] Z. Otwinowski, W. Minor, Processing of X-ray diffraction data collected in oscillation mode, Macromol. Crystallogr. Pt A 276 (1997) 307–326.
[12] G.N. Murshudov, A.A. Vagin, E.J. Dodson, Refinement of macromolecular structures by the maximum-likelihood method, Acta Crystallogr. D Biol. Crystallogr. 53 (1997) 240–255.
[13] Collaborative Computational Project, The CCP4 suite: programs for protein crystallography, Acta Crystallogr. D 50 (1994) 760–763.
[14] P. Emsley, K. Cowtan, Coot: model-building tools for molecular graphics, Acta Crystallogr. D Biol. Crystallogr. 60 (2004) 2126–2132.

[15] M.D. Winn, M.N. Isupov, G.N. Murshudov, Use of TLS parameters to model anisotropic displacements in macromolecular refinement, Acta Crystallogr. D Biol. Crystallogr. 57 (2001) 122–133.
[16] A.W. Schuttelkopf, D.M. van Aalten, PRODRG: a tool for high-throughput crystallography of protein-ligand complexes, Acta Crystallogr. D Biol. Crystallogr. 60 (2004) 1355–1363.
[17] S.C. Lovell, I.W. Davis, W.B. Arendall III, P.I. de Bakker, J.M. Word, M.G. Prisant, J.S. Richardson, D.C. Richardson, Structure validation by Calpha geometry: phi, psi and Cbeta deviation, Proteins 50 (2003) 437–450.
[18] A.A. Vaguine, J. Richelle, S.J. Wodak, SFCHECK: a unified set of procedures for evaluating the quality of macromolecular structure-factor data and their agreement with the atomic model, Acta Crystallogr. D Biol. Crystallogr. 55 (1999) 191–205.
[19] L. Urzhumtseva, P.V. Afonine, P.D. Adams, A. Urzhumtsev, Crystallographic model quality at a glance, Acta Crystallogr. D Biol. Crystallogr. 65 (2009) 297–300.
[20] D.B. Langley, A.P. Duff, H.C. Freeman, J.M. Guss, The copper-containing amine oxidase from Arthrobacter globiformis: refinement at 1.55 and 2.20 A resolution in two crystal forms, Acta Crystallogr. 62 (2006) 1052–1057.
[21] D.B. Langley, D.M. Trambaiolo, A.P. Duff, D.M. Dooley, H.C. Freeman, J.M. Guss, Complexes of the copper-containing amine oxidase from Arthrobacter globiformis with the inhibitors benzylhydrazine and tranylcypromine, Acta Crystallogr. F Struct. Biol. Cryst. Commun. 64 (2008) 577–583.
[22] M.C. Wilce, D.M. Dooley, H.C. Freeman, J.M. Guss, H. Matsunami, W.S. McIntire, C.E. Ruggiero, K. Tanizawa, H. Yamaguchi, Crystal structures of the copper-containing amine oxidase from Arthrobacter globiformis in the holo and apo forms: implications for the biogenesis of topaquinone, Biochemistry 36 (1997) 16116–16133.
[23] D.B. Langley, D.E. Brown, L.E. Cheruzel, S.M. Contakes, A.P. Duff, K.M. Hilmer, D.M. Dooley, H.B. Gray, J.M. Guss, H.C. Freeman, Enantiomer-specific binding of ruthenium(II) molecular wires by the amine oxidase of Arthrobacter globiformis, J. Am. Chem. Soc. 130 (2008) 8069–8078.
[24] S.M. Contakes, G.A. Juda, D.B. Langley, N.W. Halpern-Manners, A.P. Duff, A.R. Dunn, H.B. Gray, D.M. Dooley, J.M. Guss, H.C. Freeman, Reversible inhibition of copper amine oxidase activity by channel-blocking ruthenium(II) and rhenium(I) molecular wires, Proc. Natl Acad. Sci. USA 102 (2005) 13451–13456.